Time-series observations of ^{210}Po and ^{210}Pb radioactivity in the western North Pacific

Hajime Kawakami, Makio C. Honda, Shuichi Watanabe & Toshiro Sino

Journal of Radioanalytical and Nuclear Chemistry
An International Journal Dealing with All Aspects and Applications of Nuclear Chemistry

ISSN 0236-5731
Volume 301
Number 2

J Radioanal Nucl Chem (2014)
301:461-468
DOI 10.1007/s10967-014-3141-y

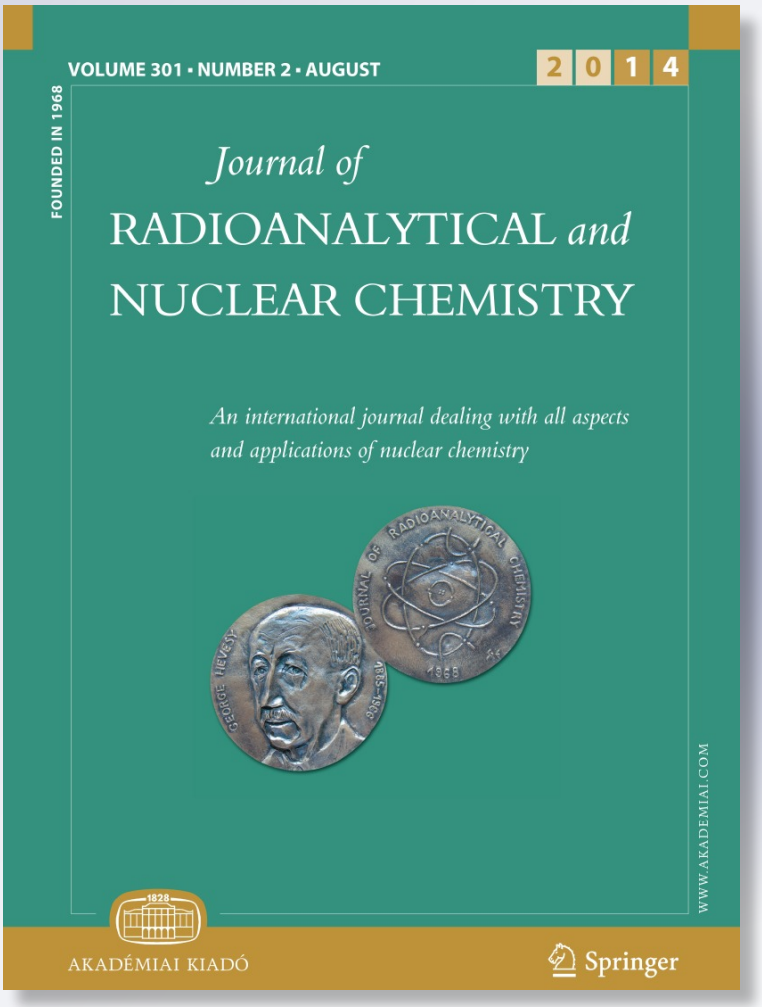

Springer

J Radioanal Nucl Chem (2014) 301:461–468
DOI 10.1007/s10967-014-3141-y

Time-series observations of ^{210}Po and ^{210}Pb radioactivity in the western North Pacific

Hajime Kawakami · Makio C. Honda · Shuichi Watanabe · Toshiro Sino

Received: 9 January 2014 / Published online: 13 April 2014

Abstract We carried out time-series observations of ^{210}Po and ^{210}Pb radioactivity in the western North Pacific Ocean. The sinking fluxes of particulate organic carbon (POC) in the mesopelagic zone were estimated from ^{210}Po radioactivity during several seasons in the subarctic and subtropical regions of the western North Pacific. The seasonal changes of POC fluxes at a depth of 400 m were larger in the subarctic region than in the subtropical region. The annual mean POC flux at a depth of 400 m was larger in the subarctic region (57 mgC m^{-2} day^{-1}) than in the subtropical region (36 mgC m^{-2} day^{-1}). The annual mean of the *e*-ratio (the ratio of POC flux to primary productivity) in the subarctic region (18 %) was about twice the *e*-ratio in the subtropical region (10 %). These results imply that the efficiency of the biological pump is larger in the subarctic region than in the subtropical region of the western North Pacific.

Keywords ^{210}Po · ^{210}Pb · North Pacific · POC flux · Mesopelagic zone

H. Kawakami (✉) · S. Watanabe
Mutsu Institute for Oceanography, Japan Agency for Marine-Earth Science and Technology, 690 Aza-kitasekine, Oaza-sekine, Mutsu 035-0022, Japan
e-mail: kawakami@jamstec.go.jp

M. C. Honda · T. Sino
Research Institute for Global Change, Japan Agency for Marine-Earth Science and Technology, 2-15 Natsushima-cho, Yokosuka 237-0061, Japan

Introduction

Global warming as a result of increases of the concentrations of greenhouse gases such as carbon dioxide in the atmosphere is of great concern to the world community. In the last few decades, the carbon cycle in the ocean has been studied to clarify the exchange of carbon dioxide between the atmosphere and the ocean. One important issue is quantification of the biological pump: namely, how much atmospheric CO_2 is assimilated by marine phytoplankton in the sunlit layer (euphotic zone) and how much carbon is exported to the ocean interior? Because the downward flux of particles decreases with increasing depth as a result of remineralization and/or grazing in the mesopelagic zone, estimation of the sinking flux of particulate organic carbon (POC) not only from the surface layer but also through the mesopelagic zone is important for assessment of the capacity of the biological pump to sequester carbon in the ocean.

Since October 2002, we have conducted time-series observations at station K2 (47°N, 160°E) in the northwestern North Pacific Ocean. High fluxes associated with the biological pump have been estimated from time series of sediment trap data [1–3] and the seasonal variability (annual amplitude) of nutrient concentrations [4, 5]. We have reported that POC fluxes from the surface layer (~100 m), as estimated from ^{234}Th, vary seasonally from 54 to 179 mgC m^{-2} day^{-1}, these fluxes greater than that found in the world ocean. Annual POC fluxes have been estimated to be about 31 g C m^{-2} $year^{-1}$ at station K2 [6]. The short-lived radionuclide ^{234}Th (half-life, 24.1 days) serves as a valuable tracer for studying the rates of particle-associated scavenging and subsequent particle export from the surface layer [7–9]. However, because ^{234}Th becomes the radioactive equivalent of ^{238}U at a depth of

Table 1 Environmental condition in stations K2 and S1 [13]

	K2	S1
Region	Subarctic	Subtropical
Sea surface temperature	Low	High
Salinity	Low	High
Nutrient	High	Low
Eolian dust input	Low (?)	High (?)
Phytoplankton abundance	High	Low

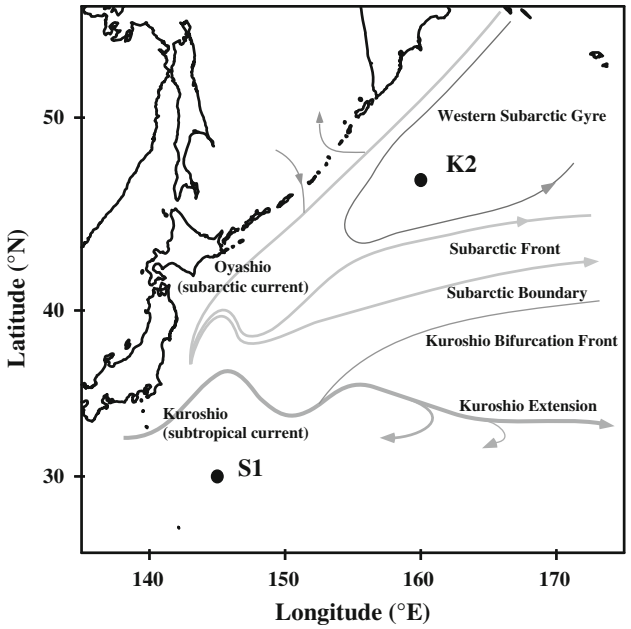

Fig. 1 Sampling stations and main ocean currents in the western North Pacific. Kuroshio and the Oyashio are the subtropical and subarctic western boundary currents in this region

approximately 100 m, ^{234}Th analysis is not suitable for estimating particle fluxes in the mesopelagic zones (200–1,000 m) of the ocean. The radioisotopes ^{210}Po and ^{210}Pb, which are not at equilibrium in the mesopelagic zone, can be used as tracers to estimate particle fluxes within that region of the water column, because ^{210}Po is preferentially removed with respect to ^{210}Pb and ingrowth constant for ^{210}Po from ^{210}Pb (0.005 day^{-1}) is not so large [10–12]. Furthermore, the ^{210}Po–^{210}Pb analysis is relatively easy to conduct because it requires only about 10 L of seawater, whereas analysis of other radionuclides (e.g. ^{228}Th and ^{230}Th) requires more than 100 L.

In addition to our observations at station K2, we started time-series observations at station S1 (30°N, 145°E) in the subtropical western North Pacific in January 2010. We hypothesized that the POC flux through the mesopelagic zone was higher at station K2 than at station S1 because stations K2 and S1 are in the eutrophic and oligotrophic regions, respectively (Table 1) [13]. In this paper, we present the seasonal changes in the vertical profiles of ^{210}Po, ^{210}Pb, and POC above a depth of 1,000 m in the subarctic and subtropical regions of the western North Pacific. We also compare the capacity of biological pump within the mesopelagic zone between the subarctic and subtropical western North Pacific.

Experimental

Sampling locations and sampling

Samples were collected at stations K2 and S1 in the western North Pacific Ocean (Fig. 1). Stations K2 and S1 are time-series stations of the Japan Agency for Marine-Earth Science and Technology [13]. Samples were collected by the research vessel (R/V) *Mirai* on four seasonal scientific cruises during autumn (October–November 2010), winter (February–March 2011), spring (April–May 2011), and summer (June–August 2011).

Two aliquots of seawater samples (10 L each) were used for determination of the radioactivities of ^{210}Po and ^{210}Pb. Duplicate samples were collected from 16 depths between 10 and 1,000 m with 12 L Niskin bottles deployed on a rosette sampler. CTD sensors (SBE 911*plus*, Sea-Bird Electronics, Inc.) attached to the rosette recorded salinity, temperature, and depth.

We used an in situ pumping system (Large Volume Water Transfer System WTS-6-1-142LV04, McLane, Inc.) to collect particulate samples for the analysis of ^{210}Po and POC content from the same depths as the seawater samples. At each depth, 200–1,000 L of seawater were filtered through a pre-combusted (450 °C, 4 h) glass-fiber filter with a nominal pore size of 0.7 μm.

Sample analysis

Immediately after collection, the seawater samples for measurements of dissolved ^{210}Po radioactivity were filtered onboard the vessel through polypropylene cartridge filters with a pore size of 0.8 μm. After filtration, the water samples were acidified to pH 1 by the addition of a concentrated HCl solution, and a ^{209}Po yield tracer with a radioactivity of approximately 1 disintegration per minute (dpm: one dpm = 1/60th Bq) and 100 mg of Fe (as $FeCl_3$) was added. After the samples were shaken and allowed to stand for about half a day, ammonium was added to the water samples to precipitate iron. The co-precipitated ^{210}Po and iron in the water samples were collected by centrifugation. To measure particulate ^{210}Po radioactivity, the filter sample collected by in situ pumping was digested with a mixture of concentrated HCl and HNO_3 (3:1, v/v) in the presence of the ^{209}Po yield

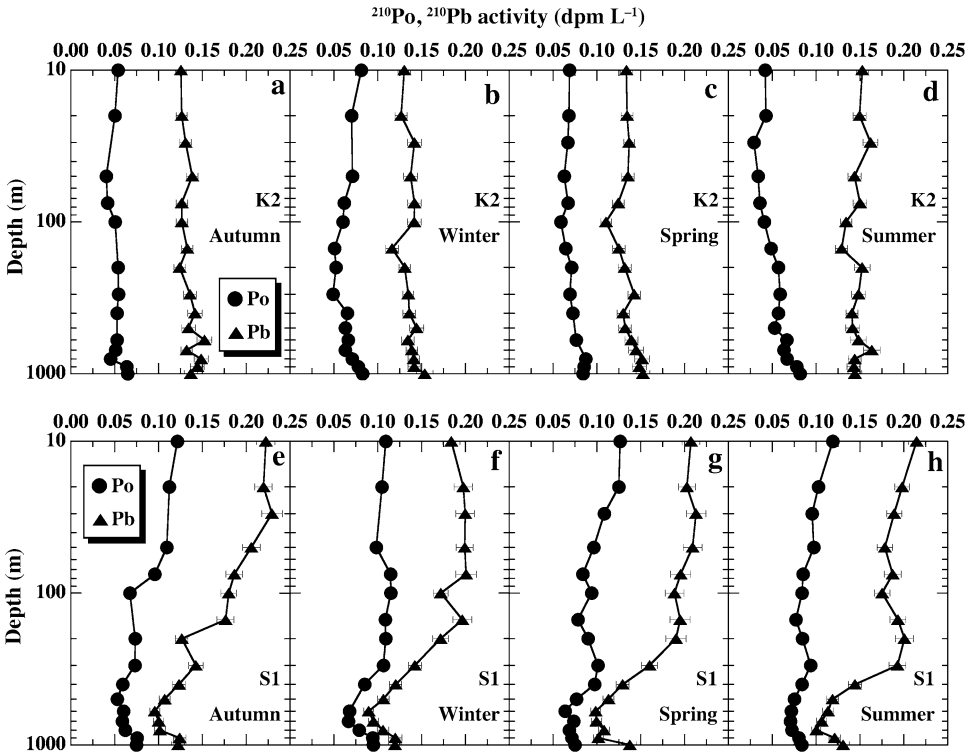

Fig. 2 Vertical distributions of total ^{210}Po and ^{210}Pb radioactivities in the subarctic (station K2, **a**–**d**) and subtropical (station S1, **e**–**h**) western North Pacific from autumn 2010 to summer 2011. Vertical axis for water depth is a logarithmic scale. The *error bars* indicate the analytical precision (1 σ) of each data point

tracer (approximately 1 dpm). Polonium separated from the seawater and particles was dissolved in approximately 50 mL of 1 M HCl, and 1–2 g of ascorbic acid was added for reduction of iron. The solution, including Po, was heated to 70–90 °C for 3 h, and the Po was adsorbed from solution onto a silver plate. The plates were alpha-counted with silicon surface-barrier detectors (Octéte, Seiko EG&G Co., Ltd.) to determine ^{209}Po and ^{210}Po activities [14, 15]. ^{210}Po activities were corrected with recovery of ^{209}Po at each sample. The recovery of ^{209}Po was usually about 50 %.

For total (dissolved and particulate) ^{210}Pb measurements, the same ^{210}Po procedure was applied to the acidified water samples stored in the airtight polyethylene container for 18 months, at which time ^{210}Po had come to radioactive equilibrium with ^{210}Pb. The repeatability errors (1 σ) for dissolved ^{210}Po, particulate ^{210}Po, and total ^{210}Pb determinations were about 4, 3, and 5 %, respectively.

For POC measurements, a stainless-steel cork borer was used to cut out subsamples with a diameter of 21 mm from the filter samples collected by in situ pumping. The subsamples were stored in a freezer until analysis. POC was measured with an elemental analyzer (Model 2400II, Perkin Elmer, Inc.). The elemental analyzer was calibrated using standard material (Acetanilide, Perkin Elmer, Inc.). Before measurement, the samples were treated with concentrated HCl vapor for 24 h to remove calcium carbonate and dried at 50 °C for 3 h. The repeatability error (1 σ) for POC was usually less than 3 %.

Results and discussion

Vertical distribution and seasonal variability of ^{210}Pb, ^{210}Po, and POC

At station K2, the total ^{210}Pb radioactivity was almost constant between depths of 10 and 1,000 m in all seasons (0.11–0.16 dpm L^{-1}) (Fig. 2). This trend was attributed to the balance between the atmospheric input of ^{210}Pb and scavenging of ^{210}Pb in the water column. The vertical and seasonal changes in total ^{210}Po radioactivity were similarly small. At station S1, the total ^{210}Pb radioactivity decreased with increasing depth (from approximately 0.2 dpm L^{-1} at 10 m to approximately 0.1 dpm L^{-1} at 800 m) during all seasons. This decreasing trend has been reported previously [16]; atmospheric input of ^{210}Pb is likely responsible for the higher total ^{210}Pb radioactivity near the surface. The total ^{210}Po radioactivity decreased slightly with increasing depth at station S1.

The total ^{210}Po radioactivity was depleted relative to total ^{210}Pb radioactivity between depths of 10 and 1,000 m at all stations. This deficiency was likely caused by scavenging of ^{210}Po by particles and subsequent downward export of those particles. At station K2, the deficiency of total ^{210}Po radioactivity relative to total ^{210}Pb radioactivity above a depth of 100 m was larger in the summer than in other seasons (Figs. 2a–d, 3a–d). At a depth of 1,000 m, the observed total ^{210}Po radioactivity was not close to

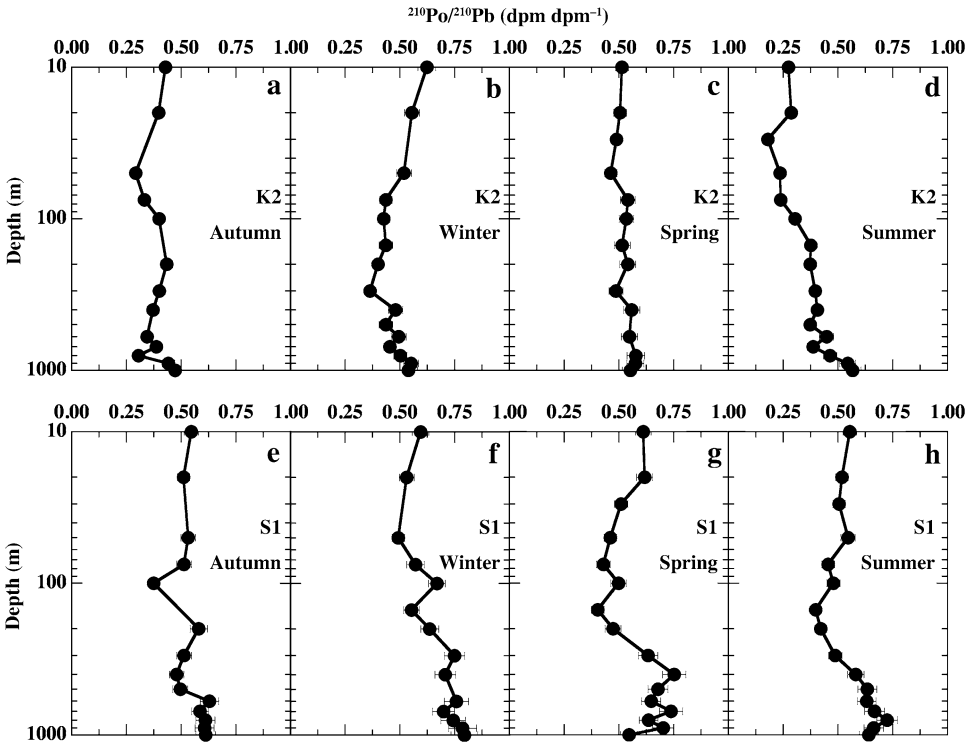

Fig. 3 Vertical distributions of ratios of total ^{210}Po to total ^{210}Pb (^{210}Po/^{210}Pb) in the subarctic (station K2, **a**–**d**) and subtropical (station S1, **e**–**h**) western North Pacific from autumn 2010 to summer 2011. Vertical axis for water depth is a logarithmic scale. The *error bars* indicate the analytical precision (1 σ) of each data point

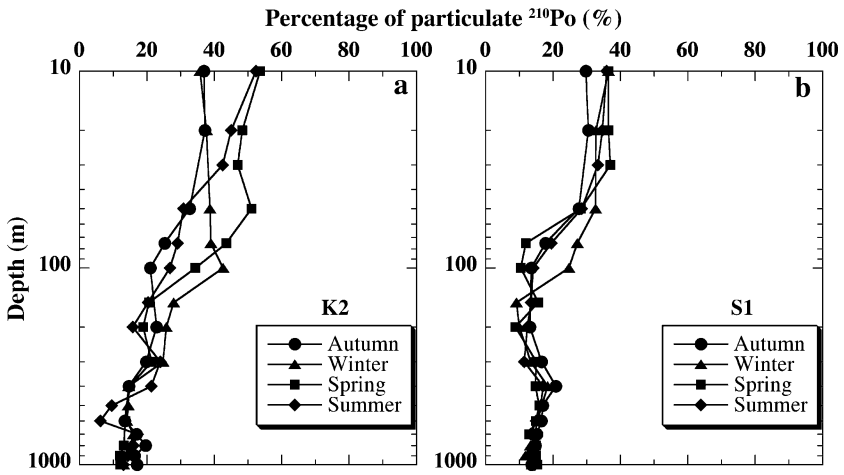

Fig. 4 Vertical distributions of percentage of total ^{210}Po accounted for by particulate ^{210}Po in the subarctic (station K2, **a**) and subtropical (station S1, **b**) western North Pacific from the autumn 2010 to summer 2011. Vertical axis for water depth is a logarithmic scale

radioactive equilibrium with total ^{210}Pb radioactivity at station K2. This disequilibrium was likely caused by not so low scavenging of ^{210}Po by the sinking particles at a depth of $\sim$ 1,000 m at station K2. In other word, the scavenging of ^{210}Po did not decreased remarkably with increasing depth at station K2. At station S1, the deficiency of ^{210}Po radioactivity was larger above 100 m than below 100 m in all seasons (Figs. 2e–h, 3e–h). At station S1, the observed radioactivities of ^{210}Po and ^{210}Pb were close to radioactive equilibrium at 1,000 m. This trend was likely due to the decrease of sinking particles and associated scavenging of ^{210}Po with increasing depth at station S1. The seasonal change in the deficiency of ^{210}Po was small at station S1. Approximately 6–54 % of the total ^{210}Po was in particulate form, and the percentages of particulate ^{210}Po to total ^{210}Po decreased with increasing depth at stations K2 and S1 (Fig. 4).

POC concentrations above 100 m changed seasonally at stations K2 and S1 (Fig. 5). The seasonal change of POC was larger at station K2 than at station S1. POC concentrations near the sea surface were largest in summer and winter at stations K2 and S1, respectively. The seasonal variations in phytoplankton biomass in the subarctic and subtropical western North Pacific are constrained within wide and narrow bounds, respectively. Furthermore, the phytoplankton biomass increases in the subarctic and

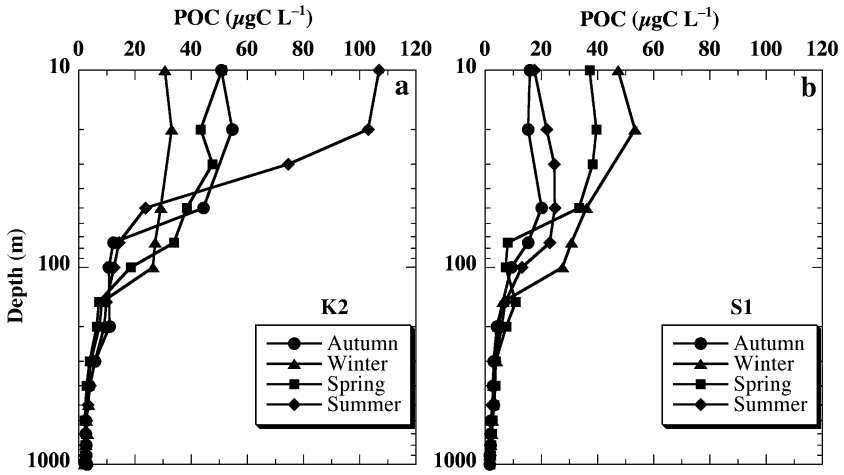

Fig. 5 Vertical distributions of POC concentrations in the subarctic (station K2, **a**) and subtropical (station S1, **b**) western North Pacific from autumn 2010 to summer 2011. Vertical axis for water depth is a logarithmic scale. The *error bars* indicate the analytical precision (1 σ) of each data point

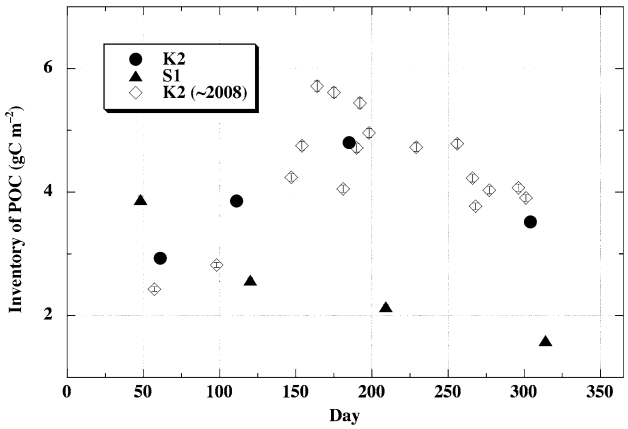

Fig. 6 Seasonal changes in the inventory of POC column-integrated from 0 to 100 m in the western North Pacific. To illustrate seasonal trends, data have been arranged from February to November, irrespective of the year of observation. The *open diamonds* are data from previous studies [6, 18]. The *error bars* indicate the analytical precision (1 σ) of each data point

subtropical western North Pacific with increasing of solar irradiance and with deepening of winter mixed layer when nutrient is supplied from the lower layer, respectively [17]. POC concentrations below 100 m were relatively small and almost constant in all seasons. POC concentrations at depths of 400–1,000 m at station K2 were slightly higher than those at station S1. We estimated the column-integrated inventory of POC between depths of 0 and 100 m. The inventories of POC at stations K2 and S1 underwent large and small seasonal changes, respectively (Fig. 6). The inventories of POC at stations K2 and S1 showed maxima in summer and winter, respectively. The seasonal changes in the POC inventory at station K2 were similar in 2010–2011 and 2002–2008 [6, 18]. The seasonal changes in inventories of POC, primary productivity, and chlorophyll *a* were comparable at station K2 [6].

The ratios of POC to particulate ^{210}Po radioactivity (POC/^{210}Po$_P$) ranged from approximately 0.14 (at ~1,000 m at stations K2 and S1) to 6.0 mgC dpm^{-1} (in the surface layer at station K2 in the summer) (Fig. 7). At station K2, POC/^{210}Po$_P$ above 100 m underwent large seasonal changes. POC/^{210}Po$_P$ below 400 m was almost constant during all seasons. At station S1, the seasonal and vertical changes in POC/^{210}Po$_P$ were small at depths of 10–1,000 m.

Sinking flux of ^{210}Po and POC

The basis of the ^{210}Po method for estimation of sinking flux is the disequilibrium between ^{210}Po and ^{210}Pb that exists in the mesopelagic zone because ^{210}Po is preferentially removed with respect to ^{210}Pb [10–12]. Assuming steady state conditions, and no effect of advective and diffusive fluxes on ^{210}Po, the sinking flux (P) and mean residence time (τ) of ^{210}Po are calculated from the following equations:

$$P = (^{210}\mathrm{Pb} - ^{210}\mathrm{Po})\lambda \quad (1)$$

$$\tau = \frac{^{210}\mathrm{Po}}{\lambda(^{210}\mathrm{Pb} - ^{210}\mathrm{Po})} \quad (2)$$

where ^{210}Pb and ^{210}Po are the measured radioactivities of total ^{210}Pb and ^{210}Po in the water column and λ is the decay constant for ^{210}Po (0.005 day^{-1}). Although temporal change of ^{210}Po activity was not zero, previous ^{210}Po studies in several oceans have assumed steady-state conditions [12, 19–23]. We calculated the sinking flux and mean residence time of ^{210}Po from ^{210}Po and ^{210}Pb radioactivities column-integrated from the sea surface down to a depth of 400 m by using Eqs. 1 and 2. We chose the depth of 400 m for two reasons: the sinking particle flux at 400 m is generally half or less of the flux from the surface layer (~100 m) [24], and 400 m in the ocean is

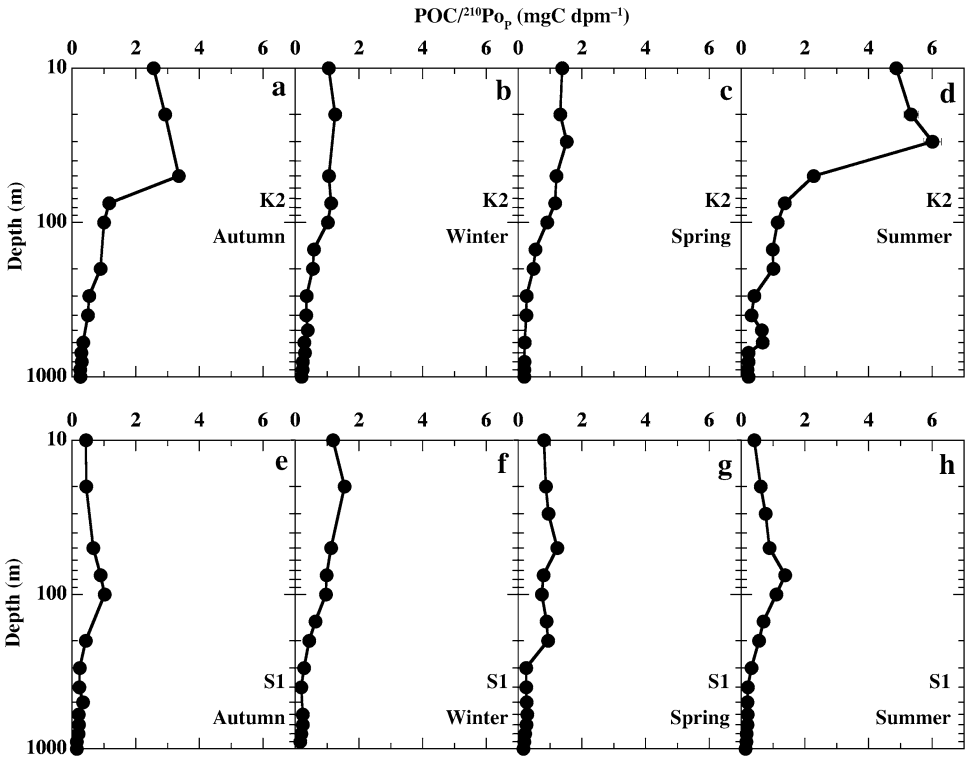

Fig. 7 Vertical distributions of ratios of POC to particulate ^{210}Po radioactivity (POC/^{210}Po$_P$) in the subarctic (station K2, **a**–**d**) and subtropical (station S1, **e**–**h**) western North Pacific from autumn 2010 to summer 2011. Vertical axis for water depth is a logarithmic scale. The *error bars* indicate the analytical precision (1 σ) of each data point

Table 2 POC fluxes estimated from ^{210}Po fluxes and ratios of POC to particulate ^{210}Po radioactivity (POC/^{210}Po$_P$), and mean residence times above a depth of 400 m in the western North Pacific

To illustrate seasonal trends, data have been arranged from February to November, irrespective of the year of observation

Station	Date	^{210}Po fluxes (dpm m^{-2} day^{-1})	POC/^{210}Po$_P$ (mgC dpm^{-1})	POC fluxes (mgC m^{-2} day^{-1})	Residence time (year)
February					
K2	26 Feb. '11	151 ± 4	0.34 ± 0.01	52 ± 2	0.42 ± 0.01
S1	16 Feb. '11	123 ± 6	0.19 ± 0.01	23 ± 1	0.94 ± 0.05
April					
K2	22 Apr. '11	128 ± 4	0.26 ± 0.01	33 ± 2	0.58 ± 0.02
S1	30 Apr. '11	167 ± 6	0.25 ± 0.01	42 ± 2	0.63 ± 0.02
July					
K2	3 Jul. '11	190 ± 5	0.33 ± 0.01	62 ± 3	0.29 ± 0.01
S1	29 Jul. '11	195 ± 6	0.21 ± 0.01	41 ± 2	0.50 ± 0.02
October–November					
K2	26 Oct. '10	161 ± 4	0.50 ± 0.02	80 ± 4	0.35 ± 0.01
S1	10 Nov. '10	163 ± 5	0.23 ± 0.01	37 ± 2	0.53 ± 0.02

close to the depth at which the POC/^{210}Po$_P$ ratio is close to a minimum (Fig. 7). At 400 m, the ^{210}Po fluxes at stations K2 and S1 were 128–190 and 123–195 dpm m^{-2} day^{-1}, respectively (Table 2).

On the basis of previous reports [12, 19–23] and the following estimates, we ignored fluxes of ^{210}Po associated with advection and diffusion. The horizontal gradient of the inventory of total ^{210}Po above 400 m at 40°N in the western North Pacific is approximately 0.3 dpm m^{-2} km^{-1} [11, 25]. Using the subsurface current velocity at 40°N in the western North Pacific (approximately 5 km day^{-1}) [26], we estimated the change of ^{210}Po activity in the western North Pacific due to horizontal advection to be no more than 2 dpm m^{-2} day^{-1}. The vertical gradients of total ^{210}Po at station S1 from spring to autumn were estimated to be approximately 5×10^{-5} dpm L^{-1} m^{-1} (increase of 0.05 dpm L^{-1} from 10 to 1,000 m, Fig. 2a, c, d) in the subsurface layer. Using the previous estimate of the annual average K_Z in the subsurface layer of the western North Pacific (3.5×10^{-5} m^2 s^{-1}) [27], the vertical diffusion flux was estimated to be approximately 0.2 dpm m^{-2} day^{-1}.

The mean residence times of ^{210}Po above a depth of 400 m at stations K2 and S1 were 0.3–0.6 and

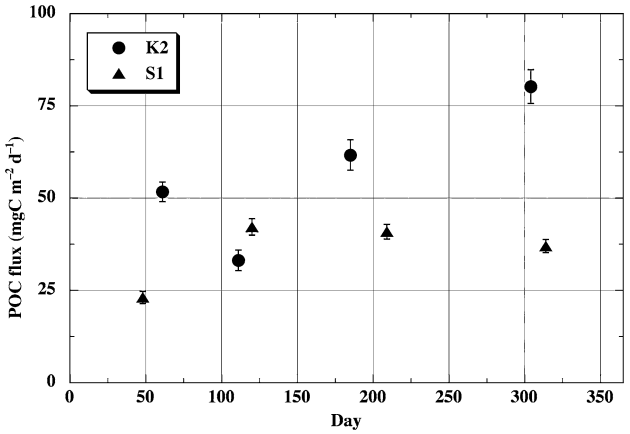

Fig. 8 Seasonal changes in POC fluxes estimated from ^{210}Po in the western North Pacific. To illustrate seasonal trends, data have been arranged from February to November, irrespective of the year of observation. The error bars indicate the analytical precision (1 σ) of each data point

0.5–0.9 years, respectively. The long mean residence time of ^{210}Po at station S1 might be attributed to releasing of ^{210}Po from particles sinking through the surface layer. These mean residence times in the western North Pacific are similar to the residence time of ^{210}Po at the Bermuda Atlantic time-series study site (0.3–0.7 years) [28].

To convert ^{210}Po radioactivity flux to a sinking flux of POC, we used the POC/^{210}Po$_P$ ratio for particles >0.7 μm at a depth of 400 m. Although it is possible that we slightly overestimated the POC/^{210}Po$_P$ ratio [12, 23], the excess POC/^{210}Po$_P$ ratio is less than 10 % [28]. Therefore, we assumed that sinking particles accounted for most of the particulate matter in the >0.7 μm size fraction in the mesopelagic zone [6, 18]. POC/^{210}Po$_P$ ratios at a depth of 400 m at stations K2 and S1 were 0.26–0.50 and 0.19–0.25 mgC dpm^{-1}, respectively (Table 2). POC fluxes at 400 m at stations K2 and S1 were 33–80 and 23–42 mgC m^{-2} day^{-1}, respectively (Table 2). The POC flux at station K2 in this study was larger than the flux previously determined from drifting sediment traps in this region (17–47 mgC m^{-2} day^{-1} at 300 m in the summer) [29]. This difference might be attributed to an overestimate of the POC/^{210}Po$_P$ ratio in this study, low trapping efficiency in the previous study, and/or the difference in seasons between this study and the previous study. POC fluxes at stations K2 and S1 underwent large and small seasonal changes, respectively (Fig. 8). POC fluxes at stations K2 and S1 showed maxima in autumn and spring, respectively. The season of maximum POC fluxes at station K2 was different between this study (autumn at 400 m) and a previous study (summer at 100 m) [6]. This difference may reflect the time lag between the passage of particles at depths of 100 and 400 m. In addition, this difference might be due to the difference in the mean lifetime of the tracers used in this study (^{210}Po, about 200 days) and previous study (^{234}Th, about 35 days) [6]. In other words, the response of ^{210}Po is slower than that of ^{234}Th.

The annual means of the POC fluxes at stations K2 and S1 were 57 and 36 mgC m^{-2} day^{-1}, respectively (Table 3). We determined primary productivity, which is the photosynthesis of organic compounds from carbon dioxide in seawater by autotrophs (e.g. phytoplankton), at stations K2 and S1 during the observation period [30], and the annual means of primary productivity at stations K2 and S1 were 309 and 369 mgC m^{-2} day^{-1}, respectively (Table 3). We estimated the *e*-ratio (the ratio of POC flux to primary productivity, that is, sinking efficiency of POC) from the POC flux at 400 m and the primary productivity in the euphotic zone (Table 3). The annual *e*-ratio at station K2 (18 %) was about twice the annual *e*-ratio at station S1 (10 %). It was thus apparent that the *e*-ratio at the subarctic western North Pacific was higher than the *e*-ratio in the subtropical region, not only in the surface layer (100 m) [6] but also the mesopelagic zone (400 m). We fitted annual means of the POC flux at 100 m (85 mgC m^{-2} day^{-1}) [6], 400 m (57 mgC m^{-2} day^{-1}; this study), and 4,810 m (3.8 mgC m^{-2} day^{-1}) [3] at station K2 to the following "Martin curve" [24]:

$$F_Z = F_{100}(Z/100)^{-b},$$

where F_Z and F_{100} are the particle fluxes at depths of Z m and 100 m, respectively. The exponent b can be used as an index of the rate of change with depth of the flux of particles. The exponent b for POC at station K2 was estimated to 0.46 ± 0.20 ($R = 0.97$), similar to the analogous value in a previous study (0.51 at 150–500 m) [29] but smaller than the analogous value in the subtropical gyre of the North Pacific (1.33 at 150–500 m) [29] and in several other oceans (0.86) [24]. These results imply that the rate of degradation of sinking POC within the mesopelagic zone was lower at station K2 than in other oceans.

Concluding remarks

The POC flux and the *e*-ratio were larger in the mesopelagic zone of the subarctic western North Pacific than in the subtropical western North Pacific. Based on the higher *e*-ratio and lower *b* exponent of the Martin curve, the rate of degradation of sinking POC was lower in the subarctic region than in the subtropical North Pacific and in other oceans.

In previous radioactivity studies using ^{234}Th as a tracer, we determined that the strength of biological pump is higher in the northwestern North Pacific than in the other oceans. In the present study, we elucidated the POC fluxes in the mesopelagic zone of the western North Pacific by a

Table 3 The annual means of POC fluxes at a depth of 400 m, primary productivity in the euphotic layer, and the *e*-ratio in the western North Pacific

	K2	S1
POC flux (mgC m^{-2} day^{-1})	57 ± 2	36 ± 2
Primary productivity[a] (mgC m^{-2} day^{-1})	309 ± 15	369 ± 18
e-Ratio (%)	18 ± 1	10 ± 1

[a] Calculated from "Database for time-series stations K2 and S1" [30]

^{210}Po–^{210}Pb radioactivity analysis. A ^{234}Th study may be insufficient to carry out a comprehensive assessment of the biological pump in the ocean. To elucidate carbon cycles throughout the water column, studies of POC fluxes in the mesopelagic and bathypelagic zones by means of ^{210}Po–^{210}Pb analysis is strongly recommended.

Acknowledgments We thank the captain, officers, and crew of the R/V *Mirai* for their help and support during the cruise. We also thank the marine technicians of the Marine Works Japan, Ltd. and Global Ocean Development, Inc. for their on-board work. This work was supported by a JSPS KAKENHI Grant-in-Aid for Young Scientists (B), Number 22710025. We also extend our profound thanks to the editor and the anonymous reviewers for their many fruitful comments.

References

1. Honda MC, Kawakami H, Sasaoka K, Watanabe S, Dicky T (2006) Geophys Res Lett. doi:10.1029/2006GL026466
2. Honda MC, Sasaoka K, Kawakami H, Matsumoto K, Watanabe S, Dicky T (2009) Deep-Sea Res I 56:2281–2292
3. Honda MC, Watanabe S (2010) Geophys Res Lett. doi:10.1029/2009GL041521
4. Honda MC, Watanabe S (2007) J Oceanogr 63:349–362
5. Kawakami H, Honda MC, Wakita M, Watanabe S (2007) J Oceanogr 63:967–982
6. Kawakami H, Honda MC (2007) Deep-Sea Res I 54:1070–1090
7. Coale KH, Bruland KW (1985) Limnol Oceanogr 30:22–33
8. Buesseler KO (1998) Global Biogeochem Cycles 12:297–310
9. Kawakami H, Yang Y-L, Honda MC, Kusakabe M (2004) Geochem J 38:581–592
10. Shimmield GB, Ritchie GD, Fileman TW (1995) Deep-Sea Res II 42:1313–1335
11. Kawakami H, Yang Y-L, Kusakabe M (2009) J Radioanal Nucl Chem 279:561–566
12. Stewart GM, Moran SB, Lomas MW (2010) Deep-Sea Res I 57:113–124
13. Research outline of Marine Biogeochemical Cycle Research Team, Japan Agency for Marine-Earth Science and Technology. http://www.jamstec.go.jp/rigc/e/ebcrp/mbcrt/. Accessed 16 Dec 2013
14. Nozaki Y (1986) Earth Planet Sci Lett 80:36–40
15. Nozaki Y, Dobashi F, Kato Y, Yamamoto Y (1998) Deep-Sea Res I 45:1263–1284
16. Nozaki Y, Turekiam KK, von Damm K (1980) Earth Planet Sci Lett 49:393–400
17. Limsakul A, Saino T, Goes JI, Midorikawan T (2002) Deep-Sea Res II 49:5487–5512
18. Kawakami H, Honda MC, Matsumoto K, Fujiki T, Watanabe S (2010) J Oceanogr 66:71–83
19. Nozaki Y, Tsubota H, Kasemsupaya V, Yashima M, Ikuta N (1991) Geochim Cosmochim Acta 55:1265–1272
20. Hong GH, Park SK, Baskaran M, Kim SH, Chung CS, Lee SH (1999) Continent Shelf Res 19:1049–1064
21. Buesseler KO, Lamborg C, Cai P, Escoube R, Johnson R, Pike S, Masque P, McGillicuddy D, Verdeny E (2008) Deep-Sea Res II 55:1426–1444
22. Verdeny E, Masqué P, Maiti K, Garcia-Orellana J, Bruach JM, Mahaffey C, Benitez-Nelson CR (2008) Deep-Sea Res II 55:1461–1472
23. Le Moigne FAC, Villa-Alfagane M, Sanders RJ, Marsay C, Henson S, García-Tenorio R (2013) Deep-Sea Res I 72:88–101
24. Martin JH, Knauer GA, Karl DM, Broenkow WW (1987) Deep-Sea Res 34:267–285
25. Kawakami H (2009) Far East J Ocean Res 2:67–82
26. Iwao T, Edoh M, Shikama N, Nakano T (2003) J Oceanogr 59:893–904
27. Andreev A, Kusakabe M, Honda MC, Murata A, Saito C (2002) Deep-Sea Res II 49:5577–5593
28. Hong GH, Baskaran M, Church TM, Conte M (2013) Deep-Sea Res II 93:108–118
29. Buesseler KO, Lmborg CH, Boyd PW, Lam PJ, Trull TW, Bidigare RR, Bishop JKB, Casciotti KL, Dehairs F, Elskens M, Honda MC, Karl DM, Siegel DA, Silver MW, Steinberg DK, Valdes J, Van Mooy B, Wilson S (2007) Science 316:567–570
30. Database for time-series stations K2 and S1, Japan Agency for Marine-Earth Science and Technology. http://ebcrpa.jamstec.go.jp/k2s1/en/. Accessed 16 Dec 2013